Current Biology, Volume *29*

Supplemental Information

Germ Granules Govern Small RNA Inheritance

Itamar Lev, Itai Antoine Toker, Yael Mor, Anat Nitzan, Guy Weintraub, Olga Antonova, Ornit Bhonkar, Itay Ben Shushan, Uri Seroussi, Julie M. Claycomb, Sarit Anava, Hila Gingold, Ronen Zaidel-Bar, and Oded Rechavi

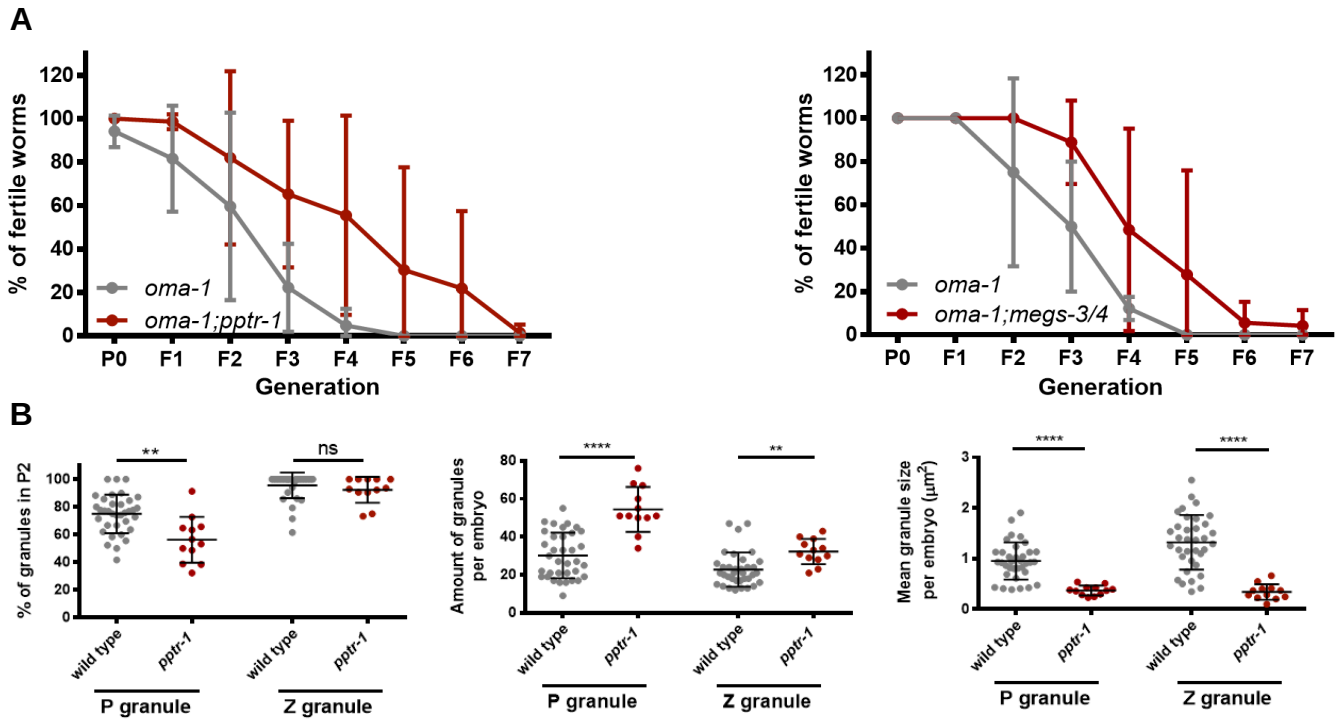

Figure S1. Mutants with defective germ granules display enhanced RNAi inheritance against the endogenous gene *oma-1*. Related to Figure 1 and 4.

(**A**) Transgenerational inheritance of silencing of a temperature-sensitive allele of the endogenous gene *oma-1*. Silencing of *oma-1* in the restrictive temperature is required for fertility. Shown are percentage of fertile worms (y-axis, mean ± SD) from six (*pptr-1)* and three (*meg-3/4*) biological replicates. In the case of *meg-3/4;oma-1*, the line originated from a cross between a mutant *meg-3/4(-/-)* male and an *oma*-1*(-/-)* hermaphrodite. For *pptr-1;oma-1* and *meg-3/4;oma-1*, obtained p values are $p<10^{-4}$ and $p<0.05$, respectively. P values were determined via Two-way ANOVA.

(B) Characterization of germ granules in *pptr*-1 embryos at the 4-cell stage. Each dot represents one analyzed embryo. All available wild-type data is displayed, and therefore appears also in Figure 5. Bars represent mean ± SD. P values were determined via Student's two-tailed t-test with Bonferroni post-hoc correction for multiple comparisons. ****- $p<10^{-4}$. **- $p<0.01$. ns- $p>0.05$.

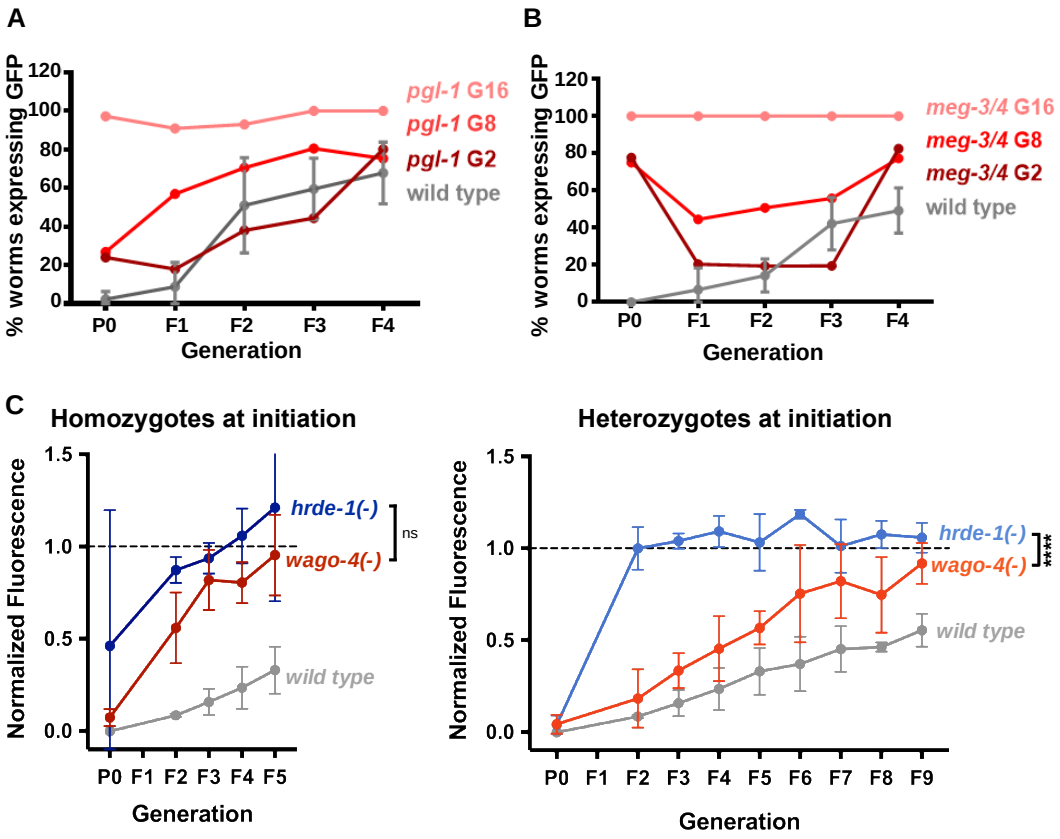

Figure S2. Transgenerational dynamics of RNAi responses in animals with mutated germ granule proteins. Related to Figure 1.

(A and B) *pgl-1* and *meg-3/4* can inherit RNAi, but lose this ability after multiple generations. Worms of the indicated genotype containing a transgene expressing *gfp* in the germline (*Pmex-5::gfp*) were exposed to *gfp* dsRNA, to initiate an RNAi response. The proportion of GFP-expressing worms (y-axis) was measured over generations (x-axis). The tested homozygous mutant strains descend from heterozygotes parents, and "G#" indicates the number of generations that have passed since homozygosity at the time of RNAi initiation. Experiments with *pgl*-1 mutants originated in a cross between *pgl*-1 hermaphrodites and wild type males expressing *Pmex-5*::gfp. Experiments with *meg-3/4* mutants originated from a cross between mutant *meg-3/4* males and wild-type hermaphrodites expressing *Pmex-5::gfp*.

(C) *wago-4* mutants can inherit RNAi if functional *wago-4* is present at the initiation stage. Homozygote (left) and heterozygote (right) worms mutated in the argonautes genes *hrde-1* (blue) and *wago-4* (red) were exposed to *gfp* dsRNA for RNAi initiation, and GFP fluorescence (y-axis) was measured over generations (x-axis). To enhance the sensitivity of the assay, the exact GFP expression levels were quantified. The heterozygote worms (right) were heterozygote only at the P0 generation, and in the next generations we measured GFP fluorescence of the homozygote mutant progeny. Fluorescence in each group was

normalized to the mean fluorescence value of the corresponding isogenic control worms originally exposed to empty vector. Shown are mean ± SD of three independent experiments, in which 25~80 animals were analyzed for each group and generation. P values were determined via Two-way ANOVA with Bonferroni post-hoc correction for multiple comparisons to *hrde-1*. ****- $p<10^{-4}$, ns- $p>0.05$. All groups were tested side by side, therefore the same wild-type group data appears on both panels.

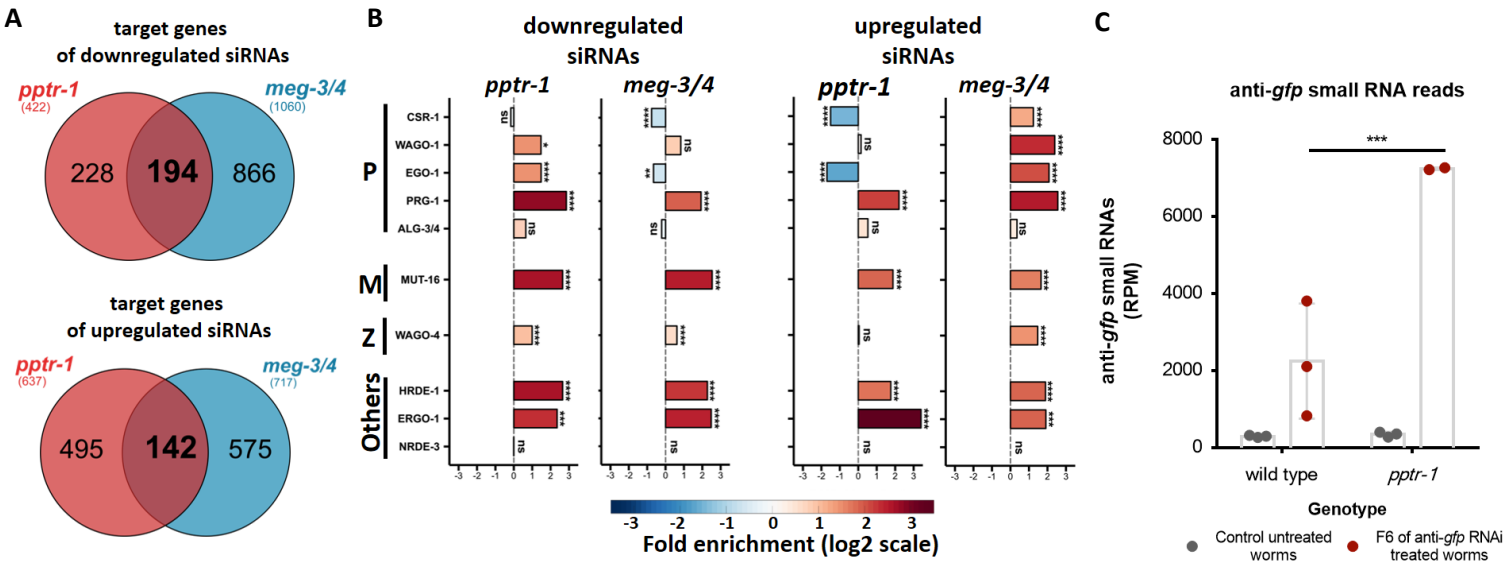

Figure S3. An analysis of endogenous and RNAi-derived small RNAs in germ granule mutants. Related to Figure 1 and Data S1.

(A) Venn diagrams representing the shared protein-coding gene targets of upregulated and downregulated small RNAs in *pptr-1* and *meg-3/4* mutants compared to wild type (analyzed via DESeq2, adjusted p-value<0.1).

(B) X-fold enrichment and depletion values (log2, bar graphs and color-coded) for genomic elements that displayed upregulated (left) or downregulated (right) expression levels of small RNA targeting them. Shown are results for genes with differential levels separately in *pptr-1* and in *meg-3/4* compared to wild type (See also Figure 1). We tested the enrichment for the list of genes differentially targeted by small RNAs against lists of genes known to be targeted by endogenous small RNAs of specific pathways (y-axis, see STAR methods for more details and a description of the statistical analysis). ****- $p<10^{-4}$, **- $p<0.01$, *- $p<0.05$.

(C) An analysis of RNAi-derived small RNAs in wild type and *pptr-1* mutants. The normalized numbers of small RNAs (reads per million) aligned to the *gfp* transgene in wild type and *pptr-1* mutants six generations after exposure to anti-*gfp* RNAi and in control untreated animals. P value was determined via Two-way ANOVA with Bonferroni post-hoc correction for multiple comparisons. ***- $p<0.001$.

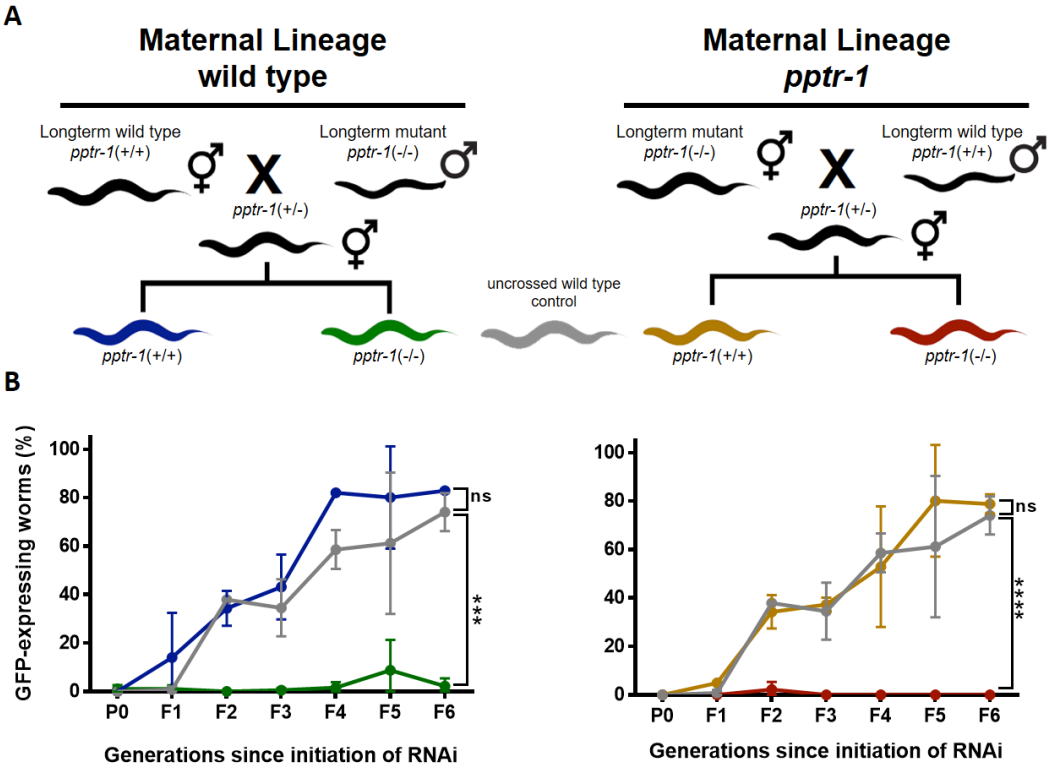

Figure S4. The function of *pptr-1* in the ancestors do not affect the ability of the progeny to inherit RNAi. Related to Figure 2.

(**A**) Schematic diagram depicting the crosses performed to determine the ancestral contribution to RNAi capacity in the descendants. Long-term *pptr-1* mutants (hermaphrodites and males) were outcrossed using wild-type worms of the opposite sex. All worms contained a transgene expressing GFP in the germline (*Pmex-5::gfp)*.

(**B**) Homozygote descendants of the crosses depicted in (A) were exposed to dsRNA complementary to *gfp*, to initiate gene silencing via RNAi. The percentage of GFP-expressing worms (y-axis, out of 40~100 worms for each group and time point) was determined over ten generations (x-axis) following exposure to RNAi. The colors depict the genotypes and lineages according to the scheme in (A). Shown are mean ± SD from two independent experiments (two independent ancestral crosses). All groups were tested side by side, and therefore the same values for the wild-type control groups are displayed on both left and right panels. P values were determined via Two-way ANOVA with Bonferroni post-hoc correction for multiple comparisons to wild type control. ****- $p<10^{-4}$, ***- $p<0.001$, ns- $p>0.05$.

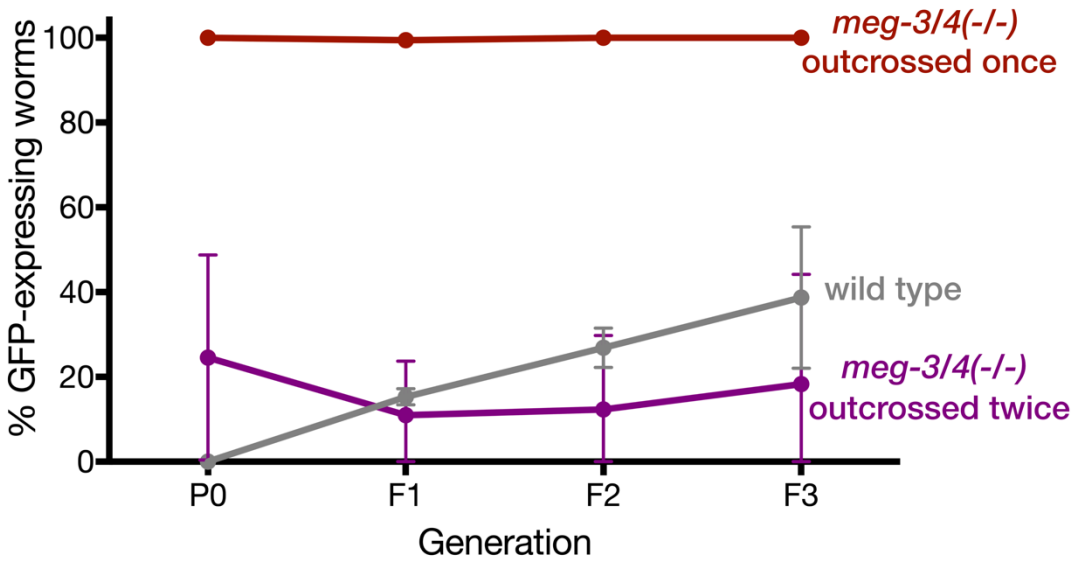

Figure S5. Repetitive crossing of *meg-3/4* mutants to wild type males leads to improvement in the capacity of the mutants to generate an RNAi response. Related to Figure 2. Worms with the indicated genotype were exposed to *gfp* dsRNA to generate RNAi two generations after homozygosity. The proportion of GFP-expressing worms (y-axis) was measured over generations (x-axis). *meg-3/4(-/-)* were outcrossed twice (purple), and tested for RNAi inheritance. Shown are mean ± SD of two independent experiments.

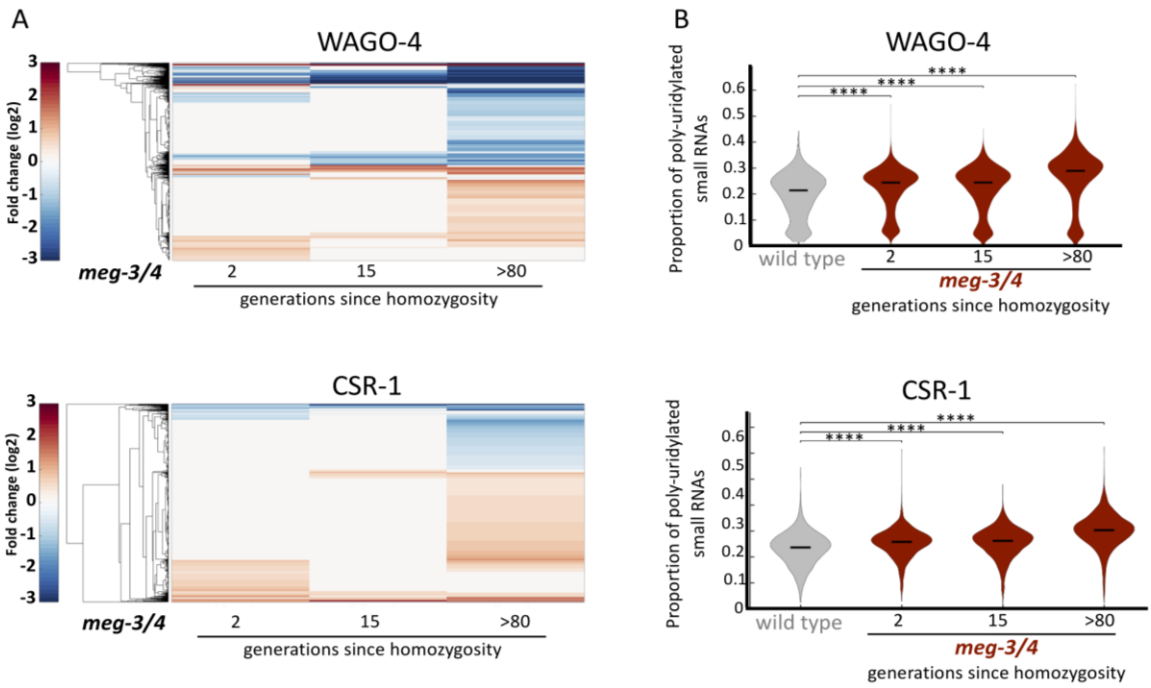

Figure S6. An analysis of transgenerationally accumulating changes in small RNA pools in *meg-3/4* mutants. Related to Figure 3.

(A) Two-way hierarchical clustering of the different examined biological groups and genes targeted by significantly differential levels of small RNAs (compared to wild type). Small RNAs samples were obtained from extracted germlines of *meg-3*/4 mutants that were homozygote for 2, 15 or >80 generations (x-axis) and derived from a cross between mutant males and wild-type hermaphrodites. Clustering diagrams of small RNAs targeting genes known to be targeted by the argonautes WAGO-4 [1] (top) and CSR-1[2] (bottom) are presented. Each row represents one gene. Only genes targeted by significantly differential levels of small RNAs in at least one sample were included in the analysis (analyzed with DEseq2, adjusted p-value<0.1). Each line is color-coded by the fold-change in expression, where lines depicting no significant differential expression appear in grey. For the >80 generations group, data from two replicates were analyzed and a third replicate was left out since it displayed substantially less read depth.

(B) An analysis of poly-uridylation of small RNAs in *meg-3/4* mutants across generations. The distribution of the average fractions of poly-uridylated small RNAs against individual genes, known to be targeted by the argonautes WAGO-4 [S1] (top) and CSR-1[S2] (bottom) are shown for each of the examined samples. Data for small RNAs samples from extracted germlines of wild type and *meg-3*/4 mutants that were homozygote for 2, 15 or >80 generations (x-axis) are shown. The fraction of poly-uridylated small RNAs was calculated as the number of reads with untemplated 3'Us out of the total aligning reads against a specific gene (only

genes with >= 5 RPM in at least one sample were included). ****- $p<10^{-4}$, ***- $p<10^{-3}$ Wilcoxon rank sum test. For the >80 generations group, data from two replicates were analyzed and a third replicate was left out since it displayed substantially less depth.

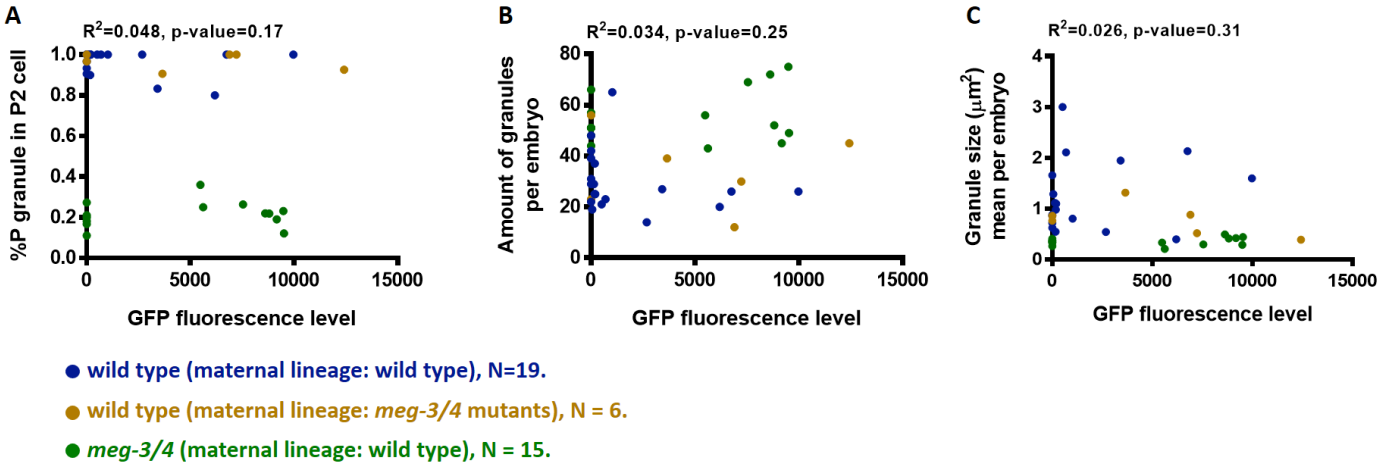

Figure S7. The level of RNAi silencing does not correlate with P granule morphology. Related to Figure 4.

Transgenic worms (*Pmex-5::gfp::h2b, pgl-1::rfp)* of the indicated genotype and lineage were exposed to anti-*gfp* dsRNA. The embryos extracted from the RNAi exposed animals were analyzed by microscopy. P granule characteristics (y-axis) are plotted against the GFP fluorescence levels (x-axis). Each dot represents one analyzed embryo. The number of analyzed embryos (N) is indicted next to the genotype. Pearson correlation scores and their P values are indicated above the panels.

References:

S1. Xu, F., Feng, X., Chen, X., Weng, C., Yan, Q., Xu, T., Hong, M., and Guang, S. (2018). A Cytoplasmic Argonaute Protein Promotes the Inheritance of RNAi. Cell Rep. *23*, 2482–2494.

S2. Claycomb, J.M., Batista, P.J., Pang, K.M., Gu, W., Vasale, J.J., van Wolfswinkel, J.C., Chaves, D.A., Shirayama, M., Mitani, S., Ketting, R.F., *et al.* (2009). The Argonaute CSR-1 and Its 22G-RNA Cofactors Are Required for Holocentric Chromosome Segregation. Cell *139*, 123–134.